

STRUCTURAL STUDY OF BIS(2,6-BIS(PYRAZOL-3-YL)PYRIDINE)NICKEL(II) BY CALORIMETRY AND EXAFS SPECTROMETRY

Kristian H. Sugiarto

Chemistry Education Department, Faculty of Mathematics and Natural Sciences
Yogyakarta State University

ABSTRACT

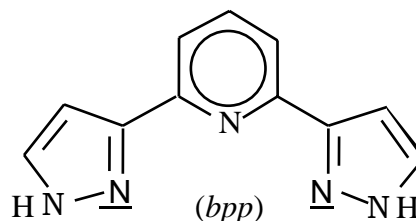
The main aim of this work is to reveal the complex formation of 2,6-bis(pyrazol-3-yl)pyridine, *bpp*, with nickel(II) perchlorate in DMF by calorimetric stepwise complex formation and then followed by EXAFS spectrometry. It was found that the complex formation follows two stepwise pathways namely the formation of mono pyrazolyl-pyridine, $[\text{Ni}(\text{DMF})_3 \text{bpp}]^{2+}$, and bis pyrazolyl-pyridine, $[\text{Ni}(\text{bpp})_2]^{2+}$; the formation constants being $\log \beta_1 = 6.57$, and $\log \beta_2 = 5.02$, and the total value of $\log \beta = 11.58$. The final formation of six-coordinated compound was confirmed by EXAFS analysis with the mean Ni-N_{bpp} bond length of 2.0646(0.0014) Å.

Keywords: nickel(II), *bpp*, EXAFS.

INTRODUCTION

The coordination property of 2,6-bis(pyrazol-3-yl)pyridine, *bpp*, since the first isolation by Lin *et al.* [1], with iron(II) was first reported in 1988 [2]. Since then, many researchers were involved in understanding the nature of the corresponding compounds in terms of spin state transition in iron(II) for system $[\text{Fe}(\text{bpp})_2]^{2+}$ [3-11]. The crystal structure of particular salts for system $[\text{Fe}(\text{bpp})_3]^{2+}$, have been confirmed by X-ray studies for the corresponding single crystal. In $[\text{Fe}(\text{bpp})_2]^{2+}$, *bpp* acts as a tridentate ligand via N_{pyrazole} - N_{pyridine} - N_{pyrazole} entity coordinated to central ion iron(II). The average Fe-N bond length is 2.174 Å for the high-spin and 1.959 Å for the low-spin.

Similarly, nickel(II) also has been reported to form $[\text{Ni}(\text{bpp})_2]^{2+}$ [2]; it is because value of the ionic radius for Ni(II) is in the range values of that for the low-spin and the high-spin Fe(II). The magnetic and electronic spectral data for the corresponding nickel(II), $[\text{Ni}(\text{bpp})_2]^{2+}$, has also been characterized, and it was indicating an octahedral complex; the structural information by X-ray data, however, has not been confirmed yet. Thus, calorimetric study of stepwise complex formation for the nickel(II)-*bpp* system in aprotic solvent, DMF, is feasible to reveal the suggested formula. The following EXAFS measurement would, then, reveal the coordination number and Ni-N bond length for the corresponding complex. This is the main aim in this work and the results are then reported in the followings.



EXPERIMENTAL

Preparation of the reagents

The pyridine, 2,6-bis(pyrazol-3-yl)pyridine, *bpp*, was synthesized as that developed by Lin *et al.* [1]. Thus, the mixture of 2,6-diacetylpyridine (~ 10 g) and N,N-dimethylformamide dimethylacetal (~20 mL) was refluxed under nitrogen flushing for about 4-8 hours. The mixture was cooled and the solvent was evaporated via rotary evaporator. The crude brown solid was dissolved in chloroform, heated with activated charcoal, filtered, and the filtrate was concentrated. The yellow solid was produced on addition of n-hexane. This solid was re-crystallized with the mixture of n-hexane-chloroform. To the suspension of the yellow solid (~ 5 g) in ethanol (~ 25 mL) and hydrazine hydrates (~ 5 mL) was stirred at room temperature for about 3-4 hours to get a clear solution. The corresponding white solid (*bpp*) was produced on dilution with water, filtered and then was re-crystallized in ethanol-chloroform. (mp. Lit. 257-259 °C).

Nickel(II) perchlorate anhydrated was prepared by removing water molecule of the hydrated. Thus, the solution of the six-hydrated nickel(II) perchlorate in acetonitrile was treated with new molecular sieves several times and then the solvent was removed by rotary evaporator [12].

N,N-dimethylformamide was dried for several weeks over molecular sieves 4A and then distilled under reduced pressure [12]. The sample, a mixture containing *btzH* and nickel(II) perchlorate by ratio 3:1 in DMF, was then inserted in a Mylar bag and this was done in dry box under nitrogen atmosphere.

Calorimetry

Calorimetric measurements were carried out by using a fully automatic on-line calorimetry system, MMC-5113, consisting of a twin-type calorimeter (Shizuoka University, Japan) [13]. Two teflon-coated stainless steel vessels each containing a test solution (40 mL) were inserted into aluminum block thermostated at $(25.0 \pm 0.0001)^{\circ}\text{C}$ in an air bath. The titrant solution was introduced into the vessels through a heat buffer by using an APB-410-20B auto piston buret. A couple of thermistors, a cooler and a heater and a tip of the autoburet were dipped in each solution. A cooler and a heater were used for adjusting temperature in the titration vessel to thermal equilibrium temperature. The temperature difference between the sample and reference vessels was measured with thermistors. By the use of two thermistors in each vessel, the temperature fluctuation within the vessel was minimized. Signals from the thermistors were amplified and were then monitored by using a digital multimeter TR6861 (Advantest). A heat capacity of the vessel is determined before each titration by using a heater and a current generator TR6142 (Advantest). When the test solution in the titration vessels reached thermal equilibrium, titration was started. The measurement was applied twice, at each titration an aliquot of 2.5 mL of a titrant solution was introduced into a (40mL) test solution. The detailed molarity of the samples are shown in Appendix.

EXAFS (Extended X-ray Absorption Fine Structure)

X-ray absorption spectra were measured in the transmission mode at the beam line BL-4 of the SR Center Ritsumeikan University (Kyoto, Japan) similar to that as described elsewhere [12]. The beam line consists of three windows, a slit, a double-crystal monochromator and two detectors. The incident X-ray intensity, I_0 , and the transmitted intensity, I , were simultaneously detected by two ionization chambers. Current signals were amplified and converted to voltage signals. The

voltage signals were finally converted to pulse frequency by the voltage-frequency conversion circuit. The pulses were measured by counter and preserved in mini-floppy disk through the microcomputer.

Measurements were repeated 1-2 times to obtain the sufficient S/N ratio. The sample solutions (nickel(II) perchlorate about 0.4 M for aqueous solution and 0.1 M nickel(II) perchlorate containing about 0.2 M *bpp* for DMF solution) were sealed in a Mylar bag in order to prevent the evaporation of solvent and to isolate from moisture. An effective jump at absorption edge was obtained by changing the number of filters. The EXAFS data were collected in transmission mode using Ge(220) monochromator crystal and ionization chambers filled with He. Data analyses were made according to a standard procedure [14]. After the background subtraction of pre-edge region by Victoreen-type function, EXAFS spectrum $k^3\chi(k)$ vs. k was extracted from the base line determination by (six) polynomial function without smoothing method or other data corrections. To obtain the local structure around nickel atom, Fourier transformation of $k^3\chi(k)$ was performed without phase-shift correction and least-squares fitting to the filtered $k^3\chi(k)$ -space was applied using the theoretical phase and amplitude functions of Mckale.

BRIEF THEORETICAL STUDY

Stepwise complex formation

Water is a good solvent for solvating anions due to its large electron-pair accepting ability, and solvation of anions are usually increased in water than that in aprotic solvents. Thus, complex formation between metal ions and anions is more favorable in aprotic solvents such as *N,N*-dimethylformamide, DMF, dimethylsulfoxide, DMSO, pyridine, and acetonitrile than in water [12, 15]. Moreover, entropies associated with formation of metal ion complexes in aprotic solvents are generally larger than those in water. In water, the water molecules in the first coordination sphere of metal ions liberated upon complexation move to well-structured bulk water and the entropy changes at two steps compensate each other. In aprotic solvents, however, the solvent molecules in the first coordination sphere may lose freedom of motion to a considerable extent due to the larger size of solvent molecules than water. The aprotic solvating molecules move to a structureless bulk solvent upon complexation, and consequently lead to a large entropy gain. Thus, the larger and more favourable entropy change of complex formation in aprotic solvents than in water may be associated

with metal ion-solvent and solvent-solvent interactions.

It has been well known that *bpp* with iron(II) forms bis-*bpp* iron(II) complex compounds, and thus acts as tridentate ligand. There is a good similarity for both iron(II) and nickel(II) in forming octahedral complex compound with the same ligand, since the value of ionic radius of nickel(II) is in the range of those for high-spin and low-spin iron(II). Thus, similarly, *bpp* and nickel(II) forms a bis-*bpp* nickel(II) complex [2]; and accordingly, the stepwise complex in DMF might involve in the following simple step of equations in Table 1.

All stepwise equations clearly shift favorably the equilibrium to the right site due to entropy factor. Each step will give characteristic heat of reaction, and thus, the stepwise complex formation constant as well as the complex formula can be determined by calorimetric measurement.

Extended X-ray Fine Structure (EXAFS)

The phenomenon of EXAFS refers to the oscillatory modulation of the X-ray absorption coefficient as a function of X-ray photon energy beyond the absorption edge [16]. The absorption, which is usually expressed in terms of absorption coefficient (β), can be determined from a measurement of the attenuation of X-rays upon their passage through a material (absorber). When the X-ray photon energy (E) is tuned to the binding energy of some core level of an atom in the material, an abrupt increase in the absorption coefficient, known as absorption edge, occurs.

Beyond the edge the absorption coefficient decreases monotonically as a function of energy for isolated atom, and the variation of absorption coefficient at energies above the absorption edge displays a fine structure called EXAFS for atoms either in a molecule or embedded in a condensed phase. Thus, EXAFS spectroscopy refers to the measurement of the X-ray absorption coefficient as a function of photon energy above the threshold of an absorption edge of an absorber. The result is an

EXAFS spectrum that generally refers to the region 40-1000 eV above the absorption edge [17].

It is now generally accepted that the EXAFS phenomenon is due to a final state interference effect involving scattering of the outgoing photoelectron from the neighboring atoms. This causes an oscillatory behavior of the absorption rate. For reasonable high energy and moderate thermal vibrations, the modulation of the absorption coefficient, which is normalized to the background absorption μ_0 , can be described in terms of the scattering amplitude from the neighboring atom $F(k)$ and the phase shift function $\Phi(k)$ which consists of contribution from the absorbing atom and the neighboring atom. If these functions are known, it should be possible to deduce structural information about the local environment of the absorber.

Data analysis composes of two major approaches, Fourier transform and the curve-fitting techniques. These result in chemical information of coordination number, Debye-Waller factor, and inter atomic distances through the assumptions of amplitude and phase transferabilities.

RESULTS AND DISCUSSION

Complex Formation

Calorimetric titration data and the detailed analysis are shown in Appendix. The data shows that the complex formation for Ni(II)-*bpp* follows two steps, the formation of the mono pyrazolyl-pyridine $[\text{Ni}(\text{DMF})_3 \text{bpp}]^{2+}$, and the bis pyrazolyl-pyridine $[\text{Ni}(\text{bpp})_2]^{2+}$, as reaction equations (1)-(3). The formation constants are 6.57, and 5.02 for $\log \beta_1$, and $\log \beta_2$ respectively, and 11.58 for the total $\log \beta$; the dominant complex is to be the bis one, $[\text{Ni}(\text{bpp})_2]^{2+}$. The main thermodynamic parameters (at 25°C) are summarized in Table 2.

Table 1 Step reaction of *bpp* and nickel (II)

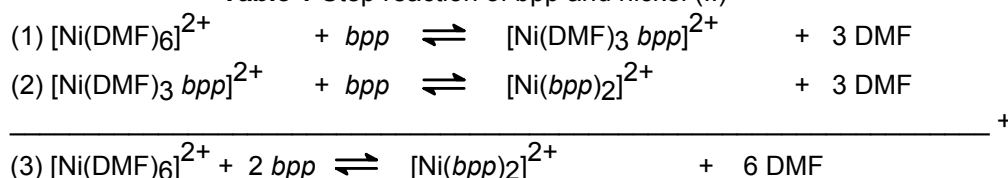


Table 2 Thermodynamics parameters of the complex (M = ion metal, L = ligand)

ML	ML	ML	Log β_n	$\Delta G/\text{kJ mol}^{-1}$	$\Delta H/\text{kJ mol}^{-1}$	$T^*\Delta S/\text{kJ mol}^{-1}$	$\Delta S/\text{J K}^{-1} \text{ mol}^{-1}$
[10]	+	[01] = [11]	6.57	-37.48	-21.90	15.58	52.26
[11]	+	[01] = [12]	5.02	-28.63	-25.86	2.77	9.29
[10]	+	2[01] = [12]	11.58	-66.11	-47.76	18.35	61.55

Thus, *bpp* acts as a merely tridentate coordinating agent of $N_{\text{pyrazole}} - N_{\text{pyridine}} - N_{\text{pyrazole}}$ about nickel(II), and this is in line with that found for the solid [2].

Structural Information

The raw EXAFS spectra and the sequent fittings to the Fourier filtered $k^3 \cdot \chi(k)$ are shown in Figure 1 for $\text{Ni}(\text{ClO}_4)_2$ in water as reference and Figure 2 for $[\text{Ni}(\text{bpp})_2]^{2+}$ in DMF. It was found that the EXAFS parameters for $\text{Ni}(\text{ClO}_4)_2$ in water are normal, the Ni–O bond length being 2.055(0.0016) Å and σ about 6.76(1.4) Å; it is a good agreement with the literature values of 2.05 (1) Å and 6.4(1) Å respectively [12]. For the complex, $[\text{Ni}(\text{bpp})_2]^{2+}$, while the coordination number was kept to be constant, 6.00, the mean Ni–N bond length was found to be 2.0646 (0.0014) Å and σ about 7.41 (0.13) Å; this value is in the range of that for $\text{Fe}_{(\text{low-spin})} - \text{N}$, 1.96 Å and $\text{Fe}_{(\text{high-spin})} - \text{N}$, 2.17 Å, in $[\text{Fe}(\text{bpp})_2]^{2+}$. Thus, the Ni–N bond length is slightly longer than Ni–O (for water) but significantly shorter than Ni–N, 2.10 and 2.11 Å, for Ni–3-Me-py and Ni–4-Me-py respectively [18]. The slightly longer of Ni–N bond length in $[\text{Ni}(\text{bpp})_2]^{2+}$ may be due to the significant bulky ligand-ligand interaction. However, the significantly shorter than that for both Ni–3-Me-py and Ni–4-Me-py distances, the monodentate moiety, suggests that *bpp* serve stronger ligand field due to the chelate character in forming the coordination compound.

CONCLUSION

Stepwise complex formation of $[\text{Ni}(\text{bpp})_2]^{2+}$ can be demonstrated *via* the formation of mono-*bpp*, and bis-*bpp* complexes by calorimetric method. The formation of the most stable and dominant bis-*bpp* complex on the final result was confirmed by EXAFS analysis, the mean Ni–N bond length in $[\text{Ni}(\text{bpp})_2]^{2+}$ being 2.0646(0.0014) Å when the coordination number was kept to be constant, six.

ACKNOWLEDGMENT

Kristian H. Sugiyarto gratefully acknowledges support for this work from Prof. Kurihara of Shizuoka University, Prof. Ozutsumi and Dr. Handa of Ritsumeikan University, and JICA.

REFERENCES

1. Lin, Y.L., and Lang, S.A., 1977, *J. Heterocycl. Chem.*, **14**, 345-347.
2. Sugiyarto, K.H., and Goodwin, H.A., 1988, *Aust. J. Chem.*, **41**, 1645 - 1663.
3. Goodwin, H.A., and Sugiyarto, K.H., 1987, *Chem. Phys. Letters*, **139**, 470 – 474
4. König, E., Kanellakopoulos, B., Powietzka, B, and Goodwin, H.A., 1989, Detailed Study of the Hysteresis Associated with the Spin-State Transition in Bis[2,6-bis(pyrazol-3-. *Inorg. Chem.*, **28**, 3993 - 3996
5. Sugiyarto, K.H., Craig, D.C., Rae, D., and Goodwin, H.A., 1994, *Aust. J. Chem.*, **47**, 869 - 890
6. Buchen, T., Gütllich, P., an Goodwin, H.A., 1994, *Inorg. Chem.*, **33**, 4573 - 4576
7. Buchen, T., Gütllich, P., Sugiyarto, K. H., and Goodwin, H.A. (1996). *Chem. Eur. J.*, **2**, 1134 – 1138
8. Sugiyarto, K.H., Weitzner, K., Craig, D.C., and Goodwin, H.A., 1997, *Aust. J. Chem.*, **50**, 869 - 873
9. Sung, R.C.W. and McGarvey, B.R., 1999, *Inorganic Chemistry*, **38**, (16), 3644-3650.
10. Sugiyarto, K.H., Scudder, M.L., Craig, D.C., and Goodwin, H.A., 2000, *Aust. J. Chem.*, **53**, 755-765
11. Sugiyarto, K.H., McHale, W.A, Craig, D.C., Rae, A.D., Scudder, M.L., and Goodwin, H.A., 2003, *J. Chem. Soc. Dalton Trans.*, 2443-2448
12. Ozutsumi, K., Koide, M., Suzuki, H. and Ishiguro, S., 1993, *J. Phys. Chem.*, **97**, 500-502.
13. Kurihara, M., Kawashima, T. and Ozutsumi, K., 2000, *Zeitschrift für Naturforschung*, **55b**, 277-284.
14. Handa, K. and Ozutsumi, K., 2002, *Memoirs of The SR Center Ritsumeikan University*, April, No. 4, (p.11-14).
15. Ozutsumi, K., Kurihara, M. and Kawashima, T., 1993, *Talanta*, **40**, (5), 599-607.
16. Teo, B. K. and Lee, P. A., 1979, *J. Am. Chem. Soc.*, **101**, 2815-2832
17. Teo, B. K., 1986, *EXAFS: Basic Principles and Data Analysis*. New York: Springer-Verlag.
18. Kurihara, Ozutsumi, K, and M., Kawashima, T., 1995, *J. Solut. Chem.*, **24**, 7, 719-734.

APPENDIX

II. AXAFS ANALYSIS

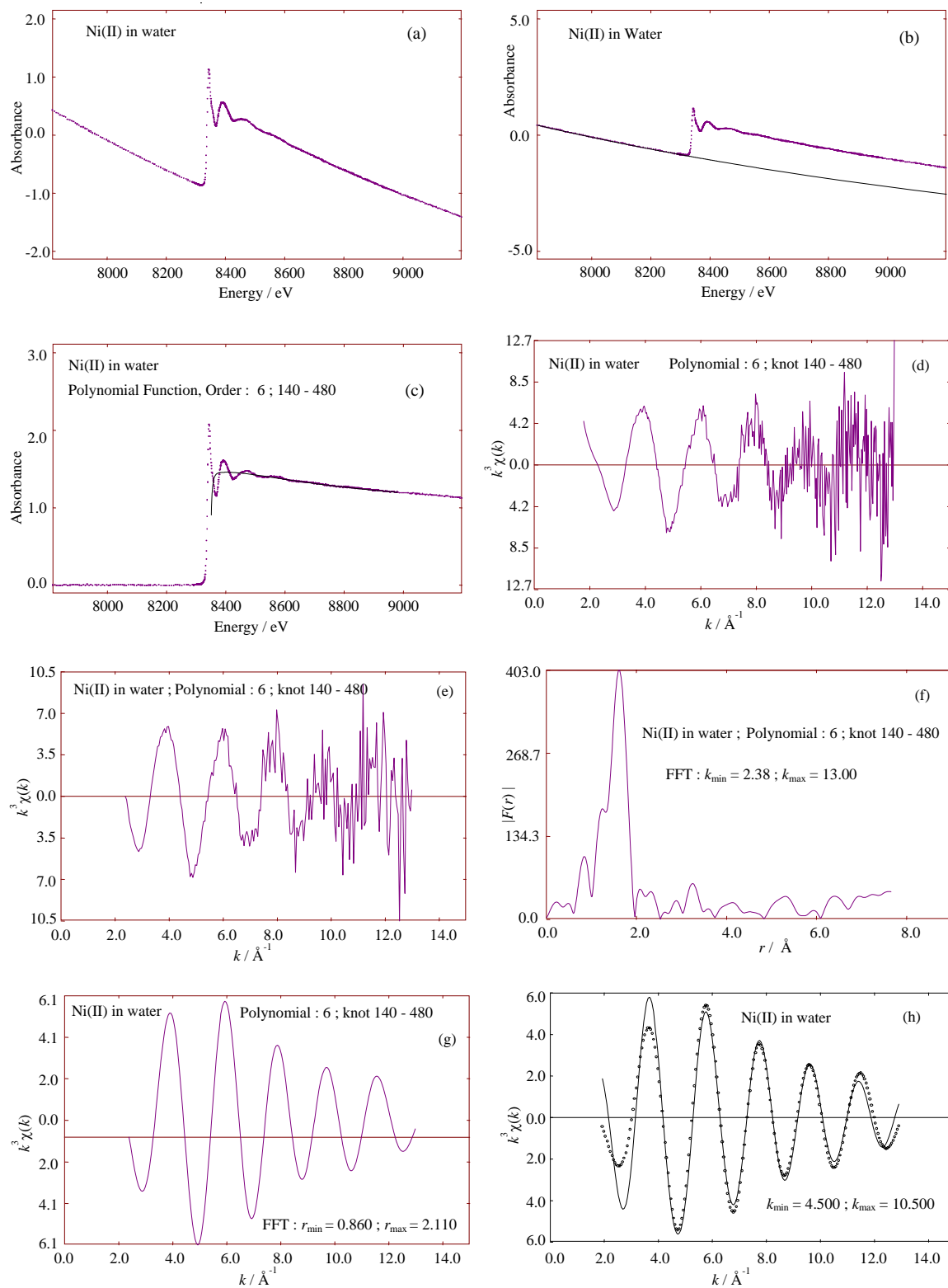


Figure 1 EXAFS Spectrum of $[\text{Ni}(\text{H}_2\text{O})_6][\text{ClO}_4]_2$ in water, (a) raw, and (b) – (h) its subsequent fittings

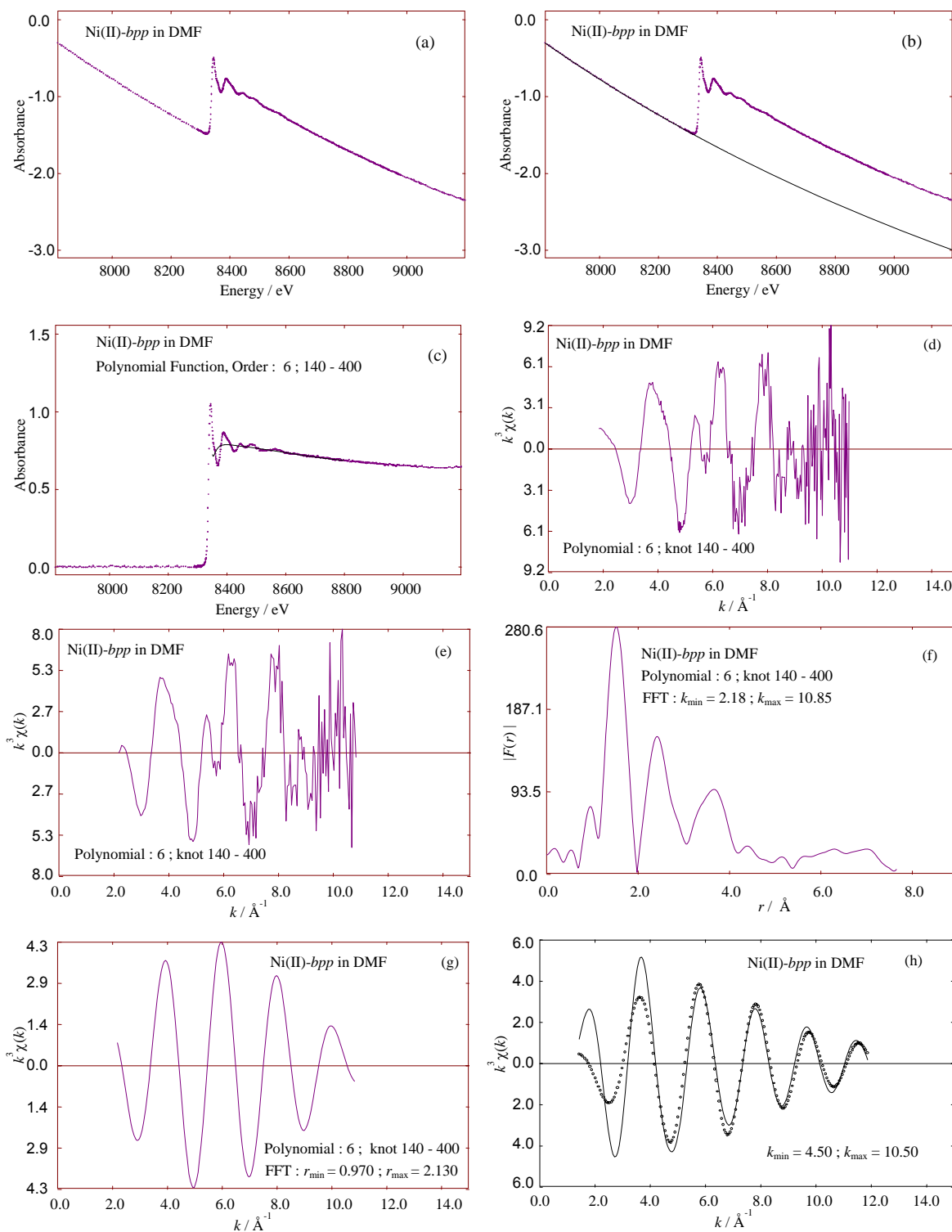


Figure 2 EXAFS Spectrum of $[\text{Ni}(\text{bpp})_2][\text{ClO}_4]_2$ in DMF, (a) raw, and (b) – (h) its subsequent fittings